A comparison of SAG mill power models

Alex Doll *
Alex G. Doll Consulting Ltd., Canada

ABSTRACT

SAG Mill power draw models are used in mill design and grinding circuit modelling to predict how much power will be consumed by a particular mill geometry and operating configuration. This paper will compare SAG mill models by Morrell, Loveday (using "Power Numbers" published by Barratt) and Austin against several published mill surveys. The purpose of the comparison is to identify the "fitting factors" used by each model and to identify which mill configurations seem to better suit each model.

The importance of conducting surveys suited to model calibration will be highlighted because the review of literature shows that survey information important to modelling is often omitted.

A recommendation for the collection of data during a mill survey is presented, along with some assumptions used by the Author in the absence of certain data. The benefit to mining companies of publishing their survey data, and thereby allowing modellers to improve their model calibration, is discussed.

The comparison of models requires a discussion of the measurement of power in a mill drive system as the models use slightly different bases for "where power is measured". The benchmarking of models against plant operations requires a similar discussion of power measurement.

*Corresponding author: Alex G Doll Consulting Ltd. PO Box 1236, Logan Lake, BC V0K1W0 Canada. Phone: +1 778-388-2444. Email: alex.doll@sagmilling.com

INTRODUCTION

Sizing the mills for a new grinding circuit requires a determination of how much energy is required for grinding (using test results such as Bond work indices) and then finding the mill sizes to draw that required amount of energy. There are several mill power draw models available to perform the second task, though generally each model is specific to a type of tumbling mill. This paper will describe three SAG mill models and compare their default results against a series of published mill surveys.

Because these models are used in the design of new plants, operating companies will benefit from improved designs (less "design fat" and risk) when consultants and model designers have better data to calibrate models against. Publishing detailed surveys will improve the models and benefit the next generation of plant designs.

METHODOLOGY

Three published models were compared to published mill survey information from industry literature. The models are run using the default values of their principal model fitting factors for comparison to the surveys, except as noted.

Austin SAG Model

The SAG mill model by proposed by Leonard Austin (1990) was largely based on modifications of earlier tumbling mill models by Hogg & Fuerstenau and F. Bond. The model is loosely structured as a kinetic and potential energy balance to describe the power draw of a mill charge. The power drawn from a cylindrical (shell-supported) mill is given by Equation 1.

$$P = KD^{2.5}L(1 - AJ_{total})\left[(1-\varepsilon_B)\left(\frac{\rho_{solids}}{w_C}\right)J_{total} + 0.6J_{balls}\left(\rho_{balls} - \frac{\rho_{solids}}{w_C}\right)\right]\phi_C\left(1 - \frac{0.1}{2^{9-10\phi_C}}\right) \quad (1)$$

Where:

- A and K are empirical fitting factors
- D is the mill diameter inside the liners, m
- J_x is the mill filling of component x, as a fraction of total mill volume (e.g. 0.3 for 30%)
- L is the mill effective grinding length, m
- P is the power evolved at the mill shell, kW
- w_C is the charge %solids, fraction by weight (e.g. 0.80 for 80%)
- ε_B is the porosity of the rock and ball bed, as a fraction of total bed volume (e.g. 0.3 for 30%)
- ρ_x is the density of a component x, t/m³
- ϕ_C is the mill speed, as a fraction of the mill critical speed (e.g. 0.75 for 75%)

The power result of the Austin model is relative to the "mill shell", also referred to as power "at the pinion".

Austin proposed a geometric factor be applied to the formula for use in cone-ended mills. The author's experience from fitting this model to published surveys suggests that Austin's factor adds too much power, and proposes that 5% extra power should be added instead (based on Barratt, Brodie & Pfeifer, 1999).

An unusual feature of Austin's model is the pulp %solids appearing in the denominator of two of the terms, meaning that the power draw drops as the pulp density increases. This is the opposite of what the other models predict – higher pulp %solids gives higher power draw in both the Loveday and Morrell models. Austin's paper recommends using a fixed value of 0.80 for this term and not varying it as the mill water addition rate changes.

Loveday/Barratt Model

Brian Loveday published a simple SAG mill model (Loveday, 1978) of the form in Equation 2. The equation uses mill dimensions (inside the liners), the density of the mill charge and an empirical "power number" that encapsulates the mill speed and volumetric filling.

$$P = P_N D^{2.5} L \rho_{Charge} \tag{2}$$

Where:

- D is the mill diameter inside the liners, m
- L is the mill effective grinding length, m
- P is the power evolved at the mill shell, kW
- P_N is an empirical "power number" which varies with mill filling and speed, unitless
- ρ_{Charge} is the density of the mill charge as given in Equation 3, t/m³

Ball charge is not explicitly used in the power formula, but is considered in the mill charge density formula:

$$\rho_{Charge} = \left[\frac{J_{balls}}{J_{total}}\rho_{balls} + \frac{J_{ore}}{J_{total}}\rho_{ore}\right] \times (1 - J_{voids}) + J_{voids}\rho_{pulp} \tag{3}$$

Where:

- J_x is the volumetric proportion of a component x (e.g. 0.2 for 20%)
- ρ_x is the density of a component x, t/m³

A chart of power numbers was published by Barratt & Sherman (2002). Values were manually extracted from this chart and smoothed by curve fitting. A subset of the power number database is shown in Figure 1.

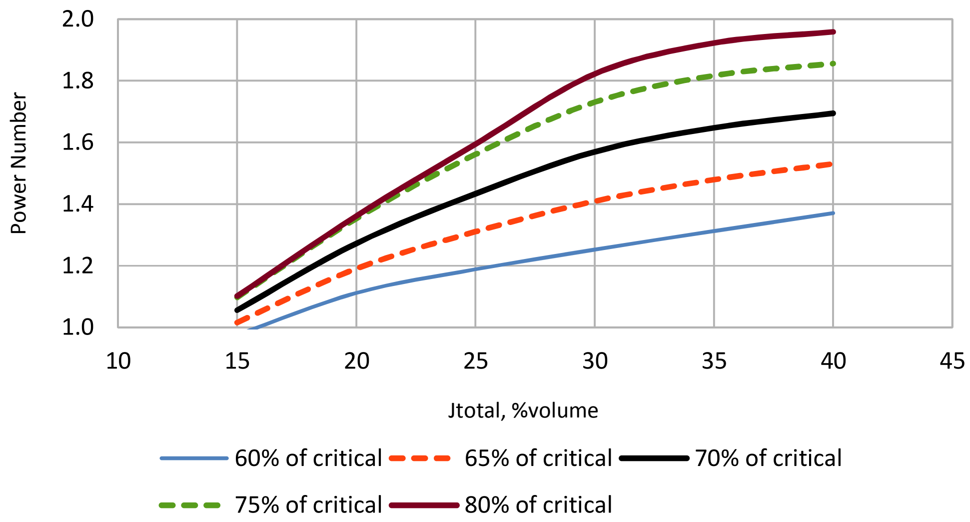

Figure 1: Power Numbers from Barratt & Sherman (2002)

The power measurement of the Loveday model is relative to the "mill shell", also referred to as power "at the pinion". The power numbers by Barratt & Sherman are fitted to "normal" cone-ended (trunnion supported) mills. For flat-ended (shell supported) mills, deduct 5% from the power draw.

Morrell C-Model

The C-model was developed by Steve Morrell at the University of Queensland as part of his PhD thesis. The Morrell C-Model is a generalised tumbling mill model and is not specific to SAG mills. The model was adopted for use in the JK SimMet™ software package and this paper is based on the description in a JK Mineral Research Centre publication (Napier-Munn et al, 1996).

The model contains too many equations and sub-equations to replicate here. In summary, the model consists of a friction balance between concentric layers within the rising part of the mill load. The model contains a great deal of physics and geometry, and uses some parameters that have been fit to laboratory or industrial scale mills. The mathematics develops the power draw of a charge geometry and motion, and then applies a fitting factor k to convert the power draw of the mill charge into the observed gross motor power (the motor input). The highly-simplified formula is given in Equation 4:

$$\textit{Gross power} = \textit{no-load power} + k \times (\textit{Charge motion power}) \tag{4}$$

The Morrell C-model provides a power draw relative to a motor input, and it must be converted to the same basis as the other models (mill shell basis) to perform meaningful comparisons. The database of mills that the published k factor was fit against consisted largely of Australian and African mills that typically have pinions (0.985 efficiency), gearboxes (0.985 efficiency) and induction motors (0.960 efficiency). Multiplying these efficiency values together suggests a conversion factor of 0.931 between motor input (C-model result) and mill shell (Doll, 2012).

EXAMPLE CALCULATION

A mill survey was published for the Meadowbank gold mine in northern Canada (Muteb & Allaire, 2013). The following criteria were identified for the May 2012 survey:

- D Diameter inside liners: 7.7 m (diameter inside shell: 26 ft)
- L Effective grinding length: 3.35 m (11 ft)
- ϕ_C Mill speed: 0.75 of critical (11.44 rpm)
- J_{total} Volumetric filling: 0.226 (22.6% v/v)
- J_{balls} Ball charge: 0.135 (13.5% v/v)
- ρ_{ore} Ore density: 2.93 t/m³
- w_C pulp density: 0.75 (75% solids)
- Grindability: A×b 38.6; Wi_{BM} 10.9 kWh/t
- Length (assumed to be flange-to-flange length): 12.4 ft
- Motor is low-speed synchronous with pinion (assume 0.9456 conversion to shell)
- Motor size: 4,760 horsepower (3,550 kW)
- Measured power draw at DCS 3,374 kW (3,190 kW at mill shell)

Liner dimensions are given as 26 rows of 9.5 inch "highs", which are assumed to be an effective thickness of 4.5 inches. The mill is trunnion supported, but the cone angle and trunnion diameter are not given.

Austin model

In addition to the published data shown above, assume the following:

- A empirical fitting factor = 1.03
- K empirical fitting factor = 10.6
- ε_B porosity of the rock and ball bed = 0.3
- ρ_{balls} density of balls = 7.8 t/m³
- w_C pulp density inside the mill charge, 80% solids (= 0.80) instead of slurry feed %solids given above.

The cylinder component of the model is described by Equation 1:

$$P = KD^{2.5}L(1 - AJ_{total})\left[(1-\varepsilon_B)\left(\frac{\rho_{solids}}{w_C}\right)J_{total} + 0.6J_{balls}\left(\rho_{balls} - \frac{\rho_{solids}}{w_C}\right)\right]\phi_C\left(1 - \frac{0.1}{2^{9-10\phi_C}}\right)$$

becomes:

$$P = (10.6)(7.7)^{2.5}(3.35)(1-(1.03)(0.226))\left[(1-0.3)\left(\frac{2.93}{0.8}\right)0.226 + 0.6(0.135)\left(7.8-\frac{2.93}{0.8}\right)\right]0.75\left(1-\frac{0.1}{2^{9-(10)(0.75)}}\right)$$

The result is 2,965 kW for the cylinder component of the mill.

The allowance for the cone section of the mill (assuming 15° cone angle) according to Austin's published method works out to 0.17, an additional 507 kW, for a total of 3,472 kW power draw at the mill shell. The measured power is 3,190 kW at mill shell, so the model predicts high by 298 kW, or 9%. However, by substituting the recommended 5% allowance for a cone end instead of Austin's cone allowance results in a 148 kW of power generated in the cone, for a total of 3,113 kW power draw at the mill shell.

The measured power is 3,190 kW, so the modified model predicts low by 78 kW, or 2%.

Loveday/Barratt model

Combining Equations 2 and 3 gives the following combined form of the Loveday power model:

$$P = P_N \times D^{2.5} \times L \times \left(\left[\frac{J_{balls}}{J_{total}}\rho_{balls} + \frac{J_{ore}}{J_{total}}\rho_{ore}\right] \times (1 - J_{voids}) + J_{voids}\rho_{pulp}\right) \quad (5)$$

From the chart in Figure 1, the value of the power number P_N for 22.6% filling and speed 75% of critical is 1.466. Assume that J_{voids} is 0.4 (different from ε_B in the Austin equation). The slurry pulp density ρ_{pulp} works out to 1.98 t/m³. Equation 5 becomes:

$$P = 1.466 \times 7.7^{2.5} \times 3.35 \times \left(\left[\frac{0.135}{0.226}7.8 + \frac{0.226-0.135}{0.226}2.93\right] \times (1-0.4) + 0.4 \times 1.98\right)$$

The result is 3,470 kW at the mill shell, which is already calibrated for a "normal" cone-ended mill. The measured power is 3,190 kW at the mill shell, so the model predicts high by 280 kW, or 9%.

Morrell C-model

The cylindrical component of Morrell's C-model gives a net power (at the charge) of 2,233 kW. The cone component requires some additional geometry for the mills: use the same assumed 15° cone angle and assume a trunnion diameter of 1.78 m (based on a ratio of other mills). The net power of the cone works out to 215 kW. The model also estimates no-load mill power of 265 kW.

Entering these net power values into Equation 4 and using the published k value of 1.26 gives:

$$\textit{Gross power} = 265 + 1.26 \times (2{,}233 + 215) = 3{,}349 \text{ kW}$$

The conversion between motor input (gross) power and mill shell power, described earlier, is 0.931. Therefore, the predicted power at the mill shell is 3,119 kW, which is 71 kW less than the measured shell power (3,190 kW), a difference of 2%.

RESULTS AND DISCUSSION

The model inputs are given in Table 1 and outputs are provided in Table 2. All models are run with their published "tuning parameters", except as noted.

- Austin model:
    - A = 1.03, K = 10.6; ε_B = 0.3
    - use a fixed pulp %solids w_C = 0.80;
    - use 5% allowance for cone ends instead of the published formula.
- Loveday/Barratt model:
    - Power numbers interpolated from Figure 1;
    - deduct 5% from predicted power in the case of flat-ended mills.
- Morrell model:
    - k=1.26 (conversion to gross power at the input of a wound-rotor induction motor);
    - J_{voids}=0.40 (different from ε_B in the Austin equation);
    - use 0.931 conversion between gross power and shell power.

Tabulation of recommended data for publication

A published mill survey would ideally provide the following information:

- D, L, J_{total}, J_{balls}, ϕ_C, ρ_{ore}, w_C and P_{DCS};
- A description of the motor and drive system and a description of where in the electrical system the DCS power indication is measured;
- Ball metallurgy (e.g. "forged steel" or "high-chrome") or ρ_{balls};
- Liner thickness estimate.

Tabulation of published surveys

The following surveys have been considered in Tables 1 & 2:

- (survey 1) Meadowbank: Muteb & Allaire (2013)
- (surveys 2 through 7) Cadia: Radziszewski & Valery (1999) and mill cone geometry from Dunne et al. (2001)
- (surveys 8 through 14) Fimiston: Nelson, Valery & Morrell (1996)
- (surveys 15 & 16) Phoenix: Lee et al. (2013)
- (surveys 17 & 18) Yanacocha: Burger et al (2011)
- (survey 19) LKAB: Bueno et al (2011)
- (surveys 20 through 25) Porgera, two sources:
    - Lam et al. (2001)
    - Grundstrom et al. (2001)

Table 1 Summary of published survey data (model inputs)

N°	Mine	*D, m*	*L, m*	J_{total}	J_{balls}	ϕ_C	ρ_{ore}	w_C	P_{DCS}, kW	conversion	P_{shell}, kW
1	Meadowbank	7.70	3.35	0.226	0.135	0.750	2.93	0.75	3,374	0.9456	**3,190**
2	Cadia *	12.02	6.10	0.288	0.000	0.790	2.60	*0.70*	11,189	0.9600	**10,741**
3	Cadia *	12.02	6.10	0.285	0.000	0.790	2.60	*0.70*	10,321	0.9600	**9,908**
4	Cadia *	12.02	6.10	0.250	0.040	0.780	2.60	*0.70*	10,824	0.9600	**10,391**
5	Cadia *	12.02	6.10	0.407	0.040	0.780	2.60	*0.70*	14,945	0.9600	**14,347**
6	Cadia *	12.02	6.10	0.316	0.120	0.740	2.60	*0.70*	17,586	0.9600	**16,883**
7	Cadia *	12.02	6.10	0.261	0.120	0.780	2.60	*0.70*	17,963	0.9600	**17,244**
8	Fimiston	10.80	4.42	0.216	0.130	0.725	2.90	0.66	9,255	0.9456	**8,752**
9	Fimiston	10.80	4.42	0.252	0.130	0.770	2.90	0.63	10,374	0.9456	**9,810**
10	Fimiston	10.80	4.42	0.222	0.115	0.800	2.90	0.60	10,976	0.9456	**10,379**
11	Fimiston	10.80	4.42	0.200	0.140	0.820	2.90	0.75	11,684	0.9456	**11,048**
12	Fimiston	10.80	4.42	0.286	0.130	0.780	2.90	0.75	11,610	0.9456	**10,978**
13	Fimiston	10.80	4.42	0.258	0.130	0.780	2.90	0.75	11,571	0.9456	**10,942**
14	Fimiston	10.80	4.42	0.190	0.120	0.800	2.90	0.75	9,408	0.9456	**8,896**
15	Phoenix	10.74	5.03	0.300	0.130	0.740	*2.70*	*0.75*	10,965	*1.0000*	**10,965**
16	Phoenix	10.74	5.03	0.270	0.130	0.740	*2.70*	*0.75*	10,304	*1.0000*	**10,304**
17	Yanacocha	9.40	9.76	0.179	0.165	0.645	2.52	0.73	12,286	*1.0000*	**12,286**
18	Yanacocha	9.40	9.76	0.229	0.191	0.631	2.52	0.80	13,992	*1.0000*	**13,992**
19	LKAB (FAG)	6.28	5.30	0.305	0.000	0.753	4.10	0.75	2,800	*0.9456*	**2,648**
20	Porgera	8.38	3.35	0.263	0.110	0.782	2.73	*0.75*	4,550	*0.9267*	**4,216**
21	Porgera	8.38	3.35	0.304	0.121	0.782	2.73	*0.75*	4,350	*0.9267*	**4,031**
22	Porgera	8.38	3.35	0.228	0.138	0.782	2.73	*0.75*	4,650	*0.9267*	**4,309**
23	Porgera	8.38	3.35	0.340	0.127	0.782	2.73	*0.75*	4,400	*0.9267*	**4,077**
24	Porgera	8.38	3.35	0.269	0.132	0.787	2.73	*0.75*	4,310	*0.9267*	**3,994**
25	Porgera	8.38	3.35	0.326	0.127	0.787	2.73	*0.75*	4,350	*0.9267*	**4,031**

* All models run with 7.80 t/m³ ball density except the Cadia surveys use 7.85 t/m³.

Assumed values for unreported parameters are indicated by italics.

Table 2 Results of models under survey conditions (model outputs)

	Austin				Loveday/Barratt		Morrell C-Model				
N°	$P_{cylinder}$ kW	P_{cone} kW	P_{shell} kW	Difference	P_{shell} kW	Difference	$P_{cylinder}$ kW	P_{cone} kW	P_{gross} kW	P_{shell} kW	Difference
1	2,965	148	**3,113**	-2.4%	**3,470**	8.8%	2,233	215	3,349	**3,119**	-2.3%
2	11,199	560	**11,759**	9.5%	**12,168**	13.3%	8,235	708	12,372	**11,521**	7.3%
3	11,131	557	**11,688**	18.0%	**12,039**	21.5%	8,179	699	12,289	**11,444**	15.5%
4	12,139	607	**12,746**	22.7%	**13,390**	28.9%	8,988	722	13,326	**12,409**	19.4%
5	14,488	724	**15,212**	6.0%	**15,096**	5.2%	11,026	1,124	16,401	**15,273**	6.5%
6	16,354	818	**17,172**	1.7%	**18,216**	7.9%	12,342	1,152	18,049	**16,807**	-0.4%
7	16,280	814	**17,094**	-0.9%	**18,505**	7.3%	12,438	1,023	18,052	**16,810**	-2.5%
8	8,580	429	**9,009**	2.9%	**9,808**	12.1%	6,245	702	9,414	**8,767**	0.2%
9	9,478	474	**9,952**	1.5%	**10,626**	8.3%	7,053	840	10,639	**9,907**	1.0%
10	8,961	448	**9,409**	-9.3%	**9,760**	-6.0%	6,668	725	10,031	**9,341**	-10.0%
11	9,456	473	**9,929**	-10.1%	**10,437**	-5.5%	7,367	743	10,950	**10,197**	-7.7%
12	9,935	497	**10,432**	-5.0%	**11,387**	3.7%	7,673	971	11,593	**10,796**	-1.7%
13	9,642	482	**10,124**	-7.5%	**11,033**	0.8%	7,413	888	11,162	**10,394**	-5.0%
14	8,591	430	**9,021**	1.4%	**9,749**	9.6%	6,563	651	9,805	**9,131**	2.6%
15	10,510	526	**11,036**	0.6%	**11,970**	9.2%	8,003	844	11,864	**11,048**	0.8%
16	10,242	512	**10,754**	4.4%	**11,765**	14.2%	7,760	775	11,471	**10,682**	3.7%
17	12,400	620	**13,020**	6.0%	**15,099**	22.9%	8,913	334	12,443	**11,587**	-5.7%
18	13,806	690	**14,496**	3.6%	**15,887**	13.5%	10,075	446	14,033	**13,067**	-6.6%
19	3,023	0	**3,023**	14.2%	**2,933** †	10.8%	2,076	0	2,842	**2,646**	-0.1%
20	3,615	181	**3,796**	-10.0%	**4,124**	-2.2%	2,780	311	4,224	**3,933**	-6.7%
21	3,876	194	**4,070**	1.0%	**4,440**	10.1%	3,011	363	4,581	**4,266**	5.8%
22	3,753	188	**3,941**	-8.5%	**4,330**	0.5%	2,886	298	4,342	**4,043**	-6.2%
23	4,024	201	**4,225**	3.6%	**4,519**	10.8%	3,146	401	4,798	**4,468**	9.6%
24	3,886	194	**4,080**	2.2%	**4,438**	11.1%	3,019	340	4,563	**4,250**	6.4%
25	4,014	201	**4,215**	4.6%	**4,521**	12.2%	3,142	391	4,782	**4,453**	10.5%

† Model power prediction reduced by 5% to account for flat-ended mill.

CONCLUSION

The Austin model is in good agreement with the surveys across a wide range of mill filling and mill speeds. It is also suitable for a typical range of ball fillings, between 8% and 18%.

- Difference between model & survey: average 2.0%; median 1.7%; standard deviation 8.3%.

The Loveday/Barratt model predicts high in most conditions surveyed and only at very high mill speeds (80% of critical and beyond) is it consistently within 8% of the surveyed power.

- Difference between model & survey: average 9.2%; median 9.6%; standard deviation 8.1%.

The Morrell C-Model is in good agreement with the surveys across a wide range of mill filling and mill speeds. It is also suitable for a typical range of ball fillings, between 7% and 18%.

- Difference between model & survey: average 1.4%; median 0.2%; standard deviation 7.4%.

Published survey information is frequently missing pulp density, a description of the electrical and drive system and an indication of how thick the liners are at the time of the survey. Including a description such as "gearless motor with DCS indicating the motor output" or "induction motor with gearbox" allows model operators to choose appropriate factors for power conversions.

ACKNOWLEDGEMENTS

Thanks to the authors of the three methods described herein for publishing their mill models with sufficient detail to permit the calculations used in this paper.

Many thanks to all the operators and authors who have published the survey data used in this paper. Without the ability to perform this sort of comparison to real operating data, all these models are nothing more than fancy mathematics.

NOMENCLATURE

A	empirical fitting factor for the Austin SAG model
D	mill diameter inside the liner, m
J_{balls}	ball filling level, as a fraction of the total mill volume (e.g. 0.10 for 10%)
J_{ore}	ore filling inside a mill, as a fraction of the total mill volume (e.g. 0.20 for 20%)
J_{total}	total filling inside a mill, as a fraction of the total mill volume (e.g. 0.30 for 30%)
J_{voids}	interstitial void space between balls and coarse rocks in a mill charge (e.g. 0.04 for 4%)
k	empirical fitting factor in Morrell C-model to convert charge power draw to motor input power draw
K	empirical fitting factor for the Austin SAG model
L	mill effective grinding length, m
P	the power evolved at the mill shell, kW
P_N	empirical "power number" for the Loveday model which varies with mill filling and speed

w_C charge %solids, fraction by weight (e.g. 0.75 for 75%)

ε_B porosity of the rock and ball bed, as a fraction of total bed volume (e.g. 0.3 for 30%)

ρ_x density of a component x, t/m³

ϕ_C mill speed, as a fraction of the mill critical speed (e.g. 0.75 for 75%)

REFERENCES

Barratt, D.J. & Sherman, M. (2002) 'Selection and Sizing of Autogenous and Semi-Autogenous Mills', *Mineral Processing Plant Design, Practice, and Control Proceedings,* Vol 1, Society for Mining, Metallurgy, and Exploration (SME), Vancouver, Canada, pp. 755–782.

Barratt, D.J., Brodie, M.N. & Pfeifer, M. (1999) 'SAG milling design trends, comparative economics, mill sizes and drives', *Bulletin of the Canadian Institute of Mining & Metallurgy,* December, pp. 62–66.

Bueno, M., Powell, M., Kojovic, T., Worth, J., Shi, F., Niva, E., Adolfsson, G., Henriksson, M., Partapuoli, Å., Wikstöm, P., Tano, K., & Fredriksson, A. (2011) 'The Dominance of the Competent', *Proceedings of the International Autogenous Grinding, Semiautogenous Grinding and High Pressure Grinding Roll Technology Conference,* Vancouver, Canada.

Burger, B., Vargas, L., Arevalo, H., Vicuna, S., Sidel, J., Valery, W., Jankovic, A., Valle, R. & Nozawa, E. (2011) 'Yanacocha Gold Single Stage SAG Mill Design, Operation, and Optimization', *Proceedings of the International Conference on Autogenous Grinding, Semiautogenous Grinding and High Pressure Grinding Roll Technology* Vancouver, B.C., Canada.

Doll, A.G. (2012), *Technical Memorandum; Mill Motor Power Definitions* Rev. 5, viewed May 17, 2013 https://www.sagmilling.com/articles/TechMemorandum-MotorPower-Rev5.pdf

Dunne, R., Morrell, S., Lane, G., Valery, W. & Hart, S. (2001) 'Design of the 40 Foot Diameter SAG Mill Installed at the Cadia Gold Copper Mine', *Proceedings of the International Conference on Autogenous and Semiautogenous Grinding Technology 2001*, Vancouver, Canada, pp. I-43–I-58

Grundstrom, C., Kanchibotla, S., Jankovich, A. & Thornton, D. (2001) 'Blast Fragmentation for Maximising the SAG Mill Throughput at Porgera Gold Mine', *Proceedings of the 27th Annual Conference on Explosives and Blasting Techniques*, ISEE, Orlando, USA.

Lam, M., Jankovic, A., Valery, W. & Kanchibotla, S. (2001) 'Maximizing SAG Mill Throughput at Porgera Gold Mine by Optimizing Blast Fragmentation', *Proceedings of the International Conference on Autogenous and Semiautogenous Grinding Technology 2001*, Vancouver, Canada, pp. I-271–I-288.

Lee, K., Bissue, C., Castillo, G., & Thies, G. (2013) 'Design and Implementation of a Brownfield SAG Pre-Crush Circuit', *Proceedings of the 45th Canadian Mineral Processors Annual General Meeting*, Ottawa, Canada, pp. 327–342.

Loveday, B.K. (1978) 'Prediction of Autogenous Milling from Pilot Plant Tests', *Proceedings of the 11th Commonwealth Mining and Metallurgical Congress,* Hong Kong.

Muteb, P. & Allaire, J. (2013) 'Meadowbank Mine Process Plant Throughput Increase', *Proceedings of the 45th Canadian Mineral Processors Annual General Meeting*, Ottawa, Canada, pp. 313–326.

Napier-Munn, T.J., Morrell, S., Morrison, R.D. & Kojovic, T. (1996) *Mineral Comminution Circuits; Their Operation and Optimisation,* Julius Kruttschnitt Mineral Research Centre, Indooroopilly, Queensland, Australia, pp. 251–272.

Nelson, M., Valery, W. & Morrell, S. (1996) 'Performance Characteristics and Optimisation of the Fimiston (KCGM) SAG Mill Circuit', *Proceedings of the International Conference on Autogenous and Semiautogenous Grinding Technology 1996*, Vancouver, Canada, pp. 233–248.

Radziszewski, P. & Valery, W. (1999) 'Cadia SAG Mill Simulated Charge Behaviour', *Proceedings of the Annual General Meeting of the Canadian Mineral Processors*, Ottawa, Canada, pp. 267–283.